



Summer 2023

Capitol Reef Ecological Conservation
Mapping Vegetation Functional Groups to Inform Invasive Vegetation Management,
Ecological Conservation and Restoration in Capitol Reef National Park

DEVELOP Technical Report

August 11th, 2023

Vanchy Li (Project Lead)
Drew Comin
Kyleigh Kowalski
Evgeny Mazko

Advisors:

Keith Weber, Idaho State University's GIS Training and Research Center (Science Advisor)
Joseph Spruce, Science Systems and Applications, Inc., Diamondhead MS (Science Advisor)

Fellow:

Ryan Healey (ID)

1. Abstract

Invasive exotic plant (IEP) species have been found within the park boundaries of Capitol Reef National Park (CARE) in Utah. Currently, remotely sensed datasets such as the Rangeland Analysis Platform (RAP) from the United States Department of Agriculture (USDA) have been used to investigate IEP species within the park, but validation of the national RAP program is necessary for informing decisions at a local scale. CARE seeks a remote monitoring solution that can precisely target managerial efforts within the park's challenging terrain and hard-to-reach locations. To fulfill this objective, we harnessed Landsat 8 Operational Land Imager (OLI) imagery and leveraged Random Forest (RF) modeling to generate classification maps characterizing vegetation functional groups for 2013 and 2022 within the park. Subsequently, the Land Change Modeler (LCM) in Idrisi TerrSet facilitated the production of a predicted classification map for 2033. The team also devised an annual grass probability map to accentuate areas impacted by exotic grasses. A comparative assessment between the RF classification map and the RAP map for 2022 revealed an overall agreement of 47.41%, with disparities primarily arising from differences in bare soil and shrub areas. Significantly, the 2022 RF-generated classification map showcased an impressive overall accuracy of 92.17%. In short, the probability map, the land cover change detection spanning 2013 to 2022, and the forecasting of observed trends into the future aids in the evaluation of invasive plant impacts and facilitation of CARE's preparedness for potential ecological disturbances. Notably, in comparison to the RAP, the RF classification method generates functional group maps that are more representative of the study area.

Key Terms

Remote sensing, invasive plants, Capitol Reef National Park, random forest, landcover, landcover change, google earth engine, supervised classification

2. Introduction

2.1 Background Information

2.1.1 Invasive & Native Plants:

Monitoring invasive plant species in Capitol Reef National Park (CARE) is critical for maintaining the park's ecological balance and integrity. Invasive exotic plants (IEPs) are non-native species that can cause significant economic and environmental harm. They can alter ecosystems at multiple scales, threaten wildlife habitats, degrade natural landscapes, and diminish recreational opportunities. There are five primary non-native species of interest to park managers at CARE: Russian thistle (*Salsola tragus*), cheatgrass (*Bromus tectorum*), halogeton (*Halogeton glomeratus*), African mustard (*Malcolmia africana*), and blue mustard (*Chorispora tenella*; Table A1).

Russian thistle is a drought-resistant annual forb with deep roots that drain soil water. It grows best in dry sandy, silty, and loamy areas, avoiding clay and shade. It prefers warmer months, blooms in mid-June, and scatters seeds as tumbleweed after shedding surface growth (Beckie & Francis, 2009). Cheatgrass, an invasive cool-season grass, invades semi-arid Western regions, germinating and dying earlier than natives, posing wildfire risks (Peterson, 2005). Halogeton, a noxious forb, alters soil and colonizes disturbed areas, often joined by cheatgrass (Pavek, 1992). African mustard and blue mustard are invasive annual forbs with similar phenological and morphological traits (Donaldson & Hanson, 2011). These annual species sprout early, outcompete natives, and dominate landscapes.

These non-native herbaceous plant species directly compete with native perennial grasses such as Indian ricegrass (*Achnatherum hymenoides*), galleta grass (*Hilaria jamesii*), alkali sacaton (*Sporobolus airoides*), blue grama (*Bouteloua gracilis*), and needle and thread (*Hesperostipa comata*) for resources and suitable habitat space. The negative effects of non-native herbaceous plant species competition is especially deleterious after habitat disturbances. Disturbances that destroy or stress native vegetation provide opportunities for invasive plants to spread because invasive annual species recover more quickly than native perennial species (Corbin & D'Antonio, 2004). Additionally, invasive plants pose a threat to native ecological communities due to their ability to spread quickly, monopolize resources, drive competition within an ecosystem, and reduce biodiversity.

Plant species can be broadly classified into functional groups based on their morphological and phenological traits. These traits can be identified and monitored across large temporal and spatial ranges by utilizing remote sensing techniques. To target the invasive exotic annual forbs and grasses of interest at CARE, this project generated maps to classify annual grass, bare soil, rock, shrub, and tree communities. Our project also created forecasted land cover maps to project future invasive plant species distribution.

2.1.2 Study Area & Period:

Our study area exists within the bounds of CARE, which is located in south-central Utah as part of the Colorado Plateau Physiographic Province, an arid region with sparse vegetation nestled between the Rocky Mountains and the Basin and Range (Figure 1). The climate of CARE is predominantly arid, characterized by an average annual precipitation of just 7.91 inches, most of which falls during the late summer monsoon season (National Park Service n.d.). The grasses that are able to survive and persist in these regions are a foundational part of the ecosystem as they are an important source of energy and nutrition in an energy-limited environment (Witwicki, 2020). Considering that disturbances from trampling and grazing are currently kept to a minimum, CARE serves as an excellent study area for observing the movement of invasive species in response to fluctuating climatic factors, such as warmer temperatures and worsening drought over time (Witwicki, 2020). Our study period spans 20 years, ranging from 2013 to 2023, and then extending to 2033 with a forecasted land cover change model.

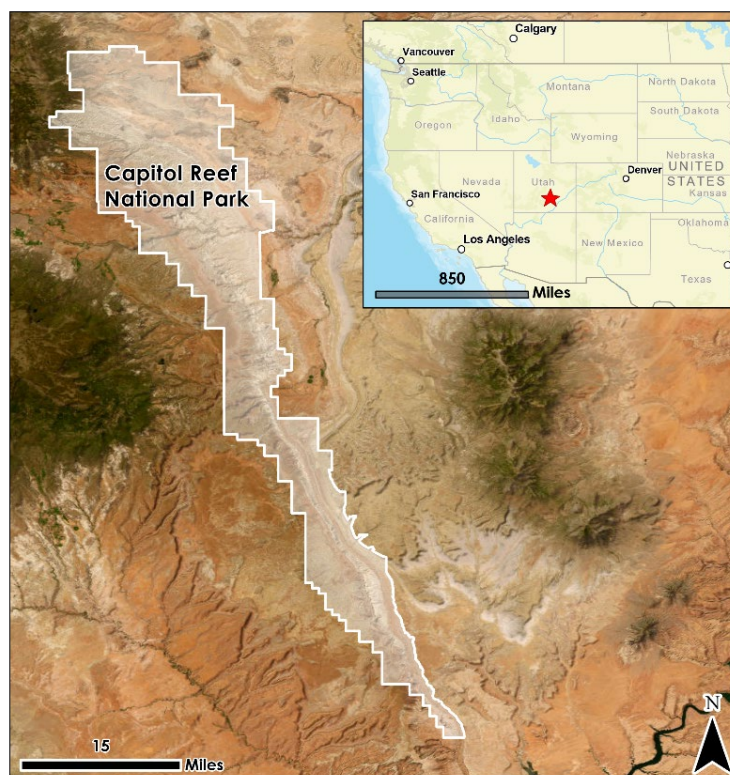


Figure 1. The location and extent of the project's study area; Capitol Reef National Park.

2.2 Project Partners & Objectives

2.2.1 Project Partners Overview

Traditionally, CARE has relied on field observations and the USDA's Rangeland Analysis Platform (RAP) for invasive plant monitoring within the park. RAP provides annual percent cover estimates of five vegetation functional groups: annual forbs and grasses, perennial forbs and grasses, shrubs, trees, and bare ground at a 30m resolution across the entire US. The estimates were produced by combining data for 75,000 field plots collected by several different agencies, along with 40 different predictor variables. The RAP recognizes its

limitations as a model-based prediction and stresses the importance of using the RAP alongside ground-truthed data and local knowledge and not as a stand-alone product for informing decision-makers (USDA Agricultural Research Service, 2023). However, the remote and rugged terrain of CARE poses challenges to conventional monitoring and data collection methods, necessitating the establishment of a more time and cost-effective remote sensing-based monitoring program.

2.2.2 Project Objectives

For this project, CARE reached out to NASA DEVELOP to investigate invasive annual species within the park, as well as to determine the validity of using the RAP to inform decisions regarding ecological conservation within CARE. This project primarily aimed to create a repeatable remote sensing methodology for mapping significant IEP species in CARE using Landsat, Sentinel, NAIP, and PlanetScope imagery. We focused on identifying invasive species like Russian thistle and Cheatgrass. Through this, we hoped to enhance our partners' understanding of these species and allow them to foster more effective control and eradication. Additionally, the project promoted knowledge enhancement and resource efficiency. Key outcomes included landcover maps, a reproducible remote monitoring process, and predictive landcover change maps to foresee invasive species spread, supporting native plant community restoration efforts.

3. Methodology

3.1 Data Acquisition

We targeted a variety of remote sensing platforms to gather data, with the selection of platforms based on their distinctive sensor capabilities and temporal resolutions. These included Landsat 8 OLI, Sentinel-2 MSI, and Dove PlanetScope imagery. In addition to remote sensing data from NASA, ESA, and Planet, we utilized several additional datasets like LiDAR from the U.S. Geological Survey (USGS) and National Agricultural Imagery from the U.S. Department of Agriculture (USDA). A large collection of ground sample data and external datasets were provided to us by our partners. The spatial extent of our study area included two image scenes of Landsat 8 OLI, four image scenes of Sentinel-2 MSI, and six image scenes of PlanetScope. The temporal range of our research spanned the years 2013 to 2023 with forecasting to 2033.

3.1.1 Remote Sensing Data

We accessed and collected Earth observations data and platforms (Table A2) primarily using Google Earth Engine (GEE) export tools and scripts. Landsat 8 OLI and Sentinel-2 MSI imagery were acquired from GEE after running several filtering processes. Initially, the collections were filtered with a custom cloud filter. Different thresholds for cloud coverage were applied based on specific requirements: less than 10% clouds for generating NDVI time series and cheatgrass amplified response analysis, and less than 0.1% for selecting imagery to create classification maps. The custom filter utilized Quality Assessment (QA) pixels from Landsat 8 OLI and the Scene Classification Map (SCL) band from Sentinel-2 MSI. This allowed us to quantify cloud pixels within the region of interest and determine the proportion of these pixels in relation to all pixels in the area. As a result, we obtained the cloud percent coverage solely for the designated area of interest. This approach led to the retrieval of over 30% more images compared to the standard cloud filters used for filtering Landsat 8 OLI or Sentinel-2 MSI images. Consequently, we were able to generate more intricate time-series data for various vegetation indexes, enabling the tracking of phenological cycles more effectively.

In addition, PlanetScope imagery was obtained through Planet Explorer directly from the Planet Labs. Acquisition dates were carefully chosen to cover the growing season, which stretches from March to October each year. This interval was specifically selected to study the vegetation life cycle within the park. For Landsat 8 OLI and Sentinel-2 MSI, imagery outside the growing season were chosen to collect winter scenes in order to trace the phenological trends across an entire year.

The primary challenge during this acquisition was high cloud coverage in certain images, leading to some data gaps. The Landsat 8 OLI data offered a spatial resolution of 30m and a temporal resolution of 16 days. Sentinel-2 MSI improved this resolution to 10m spatially and 5 days temporally, while PlanetScope brought further improvement with 1–3m spatial resolution and 1–2 days temporal resolution. We used Level 2 data

and surface reflectance products with atmospheric correction from USGS for Landsat 8 OLI and ESA for Sentinel-2 MSI.

3.1.2 Additional Datasets

To supplement the Earth observation data, we acquired additional datasets (Table A3), including National Agriculture Imagery Program (NAIP) imagery from the Utah Geospatial Resource Center and LiDAR data from the USGS. NAIP imagery has a fine spatial resolution of 0.5 – 1m and is collected biennially. It allowed us to distinguish ground features of the study area and helped to generate training sites for modeling and landcover classification more precisely. The NAIP dataset was accessed and downloaded using scripts in GEE. A second dataset acquired and processed for these purposes was the LiDAR data for Southern Utah and Kane County. The quality levels (QL) of the dataset contained 1m QL2 and QL1 data used to create a high-resolution topographic map and generate additional surface derivatives like slope and aspect. With LiDAR, our team was also able to process the imagery and classify it by height which better distinguished trees from shrubs.

3.1.3 Ground Sample Data

Our partners provided polygons and points from vegetation field surveys conducted between 2001 and 2023. Some polygons represented plots containing information on invasive species and percent coverage of plants and bare soils within each plot, while other polygons were a blend of field observations and office observations utilizing imagery or secondhand reports. Point data contained coordinates for documented invasive species. Supplementary datasets were also provided by our partners such as geological maps, soil maps, vegetation maps, spring and seep point locations, historical grazing data, hiking trails, and park road data. Many of the partner provided polygons were not evenly distributed throughout the study area and instead were concentrated in two specific regions of the park: the Uplands and Sandy 3 regions. We assume that this clustering is occurring in regions of the park that are relatively easier to access, which means that our classification maps may be slightly more representative of these types of landscapes than parts of the park that are more rugged and difficult to access.

3.2 Data Processing

3.2.1 Earth Observation Data

After applying a cloud filter, we merged the selected Landsat and Sentinel images into a unified mosaic for each individual date. The overlap areas have been handled by Google Earth Engine on the principle of the first image. This mosaic encompassed two Landsat 8 OLI scenes and four Sentinel-2 MSI granules, covering the full extent of CARE. Additionally, our team visually inspected the mosaics to confirm the accuracy of cloud coverage percentages and to ensure that scenes appeared identical for the same date. Additionally, a scaling factor was applied to the Sentinel-2 MSI imagery using a division of 10,000, as per the ESA documentation. For Landsat 8 OLI, the scaling involved multiplying each band by 0.0000275 and then subtracting 0.2, following the guidelines from the USGS documentation.

The resulting image collection underwent further processing to compute various vegetation indices. This was achieved using raster band calculation capabilities within GEE. The following indices were calculated (Table A4) in GEE: Normalized Difference Vegetation Index (NDVI), Enhanced Vegetation Index (EVI), Modified Soil Adjusted Vegetation Index (MSAVI2), and Normalized Difference Moisture Index (NDMI). The resulting indices were added as bands to the mosaicked collection. Finally, processed images were clipped to the boundaries of the CARE and downloaded for further analysis. The PlanetScope data were also filtered to identify cloudless images. Using the same methodology, we filtered, mosaicked, and clipped the data using GEE. Following these steps, we also computed the NDVI and appended it as an additional band to the image collection.

3.2.2 Additional Datasets

To create a mosaicked LiDAR dataset, we converted LAZ files into 7,222 LAS files using the LAsTools toolkit in ArcGIS Pro with additional clipping of the dataset to the boundaries of our study area. LAsTools

offers a specialized tool for classifying LiDAR points based on their height, enabling them to access the height above ground data. Once points were classified, we converted the LiDAR point cloud to a raster so it could be further analyzed. With the raster layer we classified anything with a height above 3 meters as trees and anything that is more than 0.3 meters and less than 3 meters as shrubs. Similarly, the NAIP imagery was mosaicked and clipped to the boundaries of the study region.

One of the issues with the generated raster layer was that steep slopes and cliffs were also being classified as trees in many cases. To remove the cliffs, we used the slope map generated from the LiDAR elevation data to remove points classified as trees with a slope over 50%. This fixed most of the inconsistencies in our data, but there were still some slopes that were less than 50% that did not have trees that were showing up as trees in the data. To correct for these areas, we used NDVI values to remove any areas that had an NDVI less than 0. This effectively removed all of the cliff areas that were being classified as trees in the data and allowed us to use this raster dataset to create training and validation sites.

3.2.3 In-Situ Data and Training Sites

The training and validation polygons were processed and combined by using in-situ data and additional observations from the NAIP and LiDAR datasets. The data provided by partners could be divided into several different types based on the source of observations. Initial invasive plants field survey data contained robust attribute tables with useful columns such as invasive species, severity, distribution, and notes, as well as occasionally containing approximate estimates of the percent coverage for the polygon. To extract meaningful polygon data from these data, we filtered all the polygons with moderate and high severity and percent coverage of more than 50% to add to the training data. Northern Colorado Plateau Network polygons had several tables associated with them with information about land percent coverage and its type (Bare Soil, species of grasses, trees and etc.). The Assessment, Inventory, and Monitoring plots provided by our partners contained raw data from the field surveys that have been used to calculate approximate percent cover for each plot. After those calculations, the same logic that has been applied for the previous polygons was applied for the newly calculated data (Appendix B).

Resulting polygons had additional information associated with them such as: general type (e.g., grass/forb, tree/shrub.), functional group (e.g., annual grass, tree, shrub, bare soil), and species (e.g., cheatgrass, Russian thistle, halogeton). Most of the generated polygons were bare soil with grasses. To enrich the training sites with groups underrepresented in the in-situ data (trees, shrubs, rocks) we added newly created polygons by inspecting NAIP imagery and LiDAR generated heights rasters for the areas with visual prevalence of those types (Figure 2).

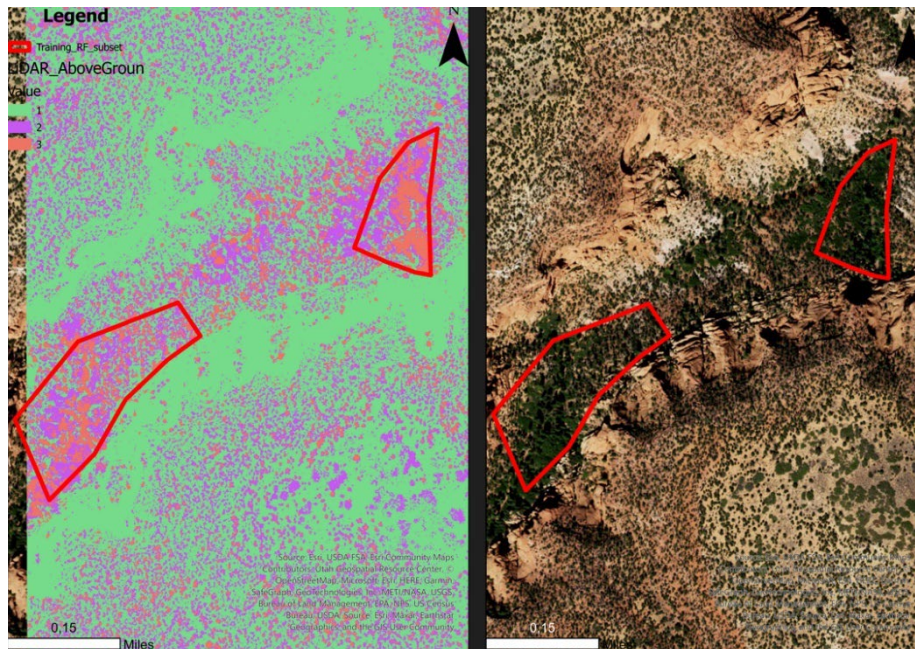


Figure 2. Visual detection and verification of training samples based on NAIP (right) and LiDAR heights raster (left). Inspecting NAIP image we can identify areas with high percentage of woody plants, but we can't quite distinguish between them directly since those two types appears to be pretty similar on the planar view. The LiDAR data adds the third dimension and helps us to distinguish between them by using classification based on the height of the feature. The purple values on the left correspond to the shrubs, or features with height between 0.3 m and 3 m, and orange represents trees or features with height more than 3 m.

3.2.4 RAP Data

The RAP provides continuous vegetation cover for five vegetation functional groups: annual grass, perennial grass, bare ground, shrub, and tree (USDA Agricultural Research Service, 2023). In order to compare the RAP data to our Random Forest classifications, these five functional group layers were compiled into a single raster layer. All five continuous cover layers from 2022 were retrieved from the RAP and compiled into a single raster by identifying the functional group with the highest estimated percent cover for each pixel using a series of raster calculator conditional (CON) statements. A sixth class was generated to represent all pixels for which there were two or more landcover classes that tied for the highest estimated percent cover for a single pixel. The pixels assigned to "Tied" were then re-classified into the classes assigned to the majority of nearby pixels. Finally, due to the absence of perennial in-situ data for training the Random Forest classification, the RAP annual grass and perennial grass classes were reclassified into a single class "Grass". Similarly, our Random Forest classes of "Rock" and "Bare Soil" were re-classified into a single class, "Bare Ground". The final maps of Random Forest and RAP classifications consisted of four classes: Grass, Bare ground, Shrub, and Tree to facilitate a direct comparison between these classifications.

3.3 Data Analysis

3.3.1 Spectral Signatures

Before running Random Forest, we obtained spectral signatures to detect the differences or similarities between each class. The distinguishability of spectral signatures played a crucial role in the accuracy of supervised classification methods. Using the SIGCOMP function in Idrisi TerrSet, we generated the spectral signature plot for six types: annual grass, perennial grass, rock, bare soil, shrub, and tree.

Upon analyzing the plot (Figure B1), we observed that rock, shrub, and tree signatures are most distinct and easily separable. However, the spectral signature of perennial grass showed similarities with both annual grass and bare soil, making it difficult to differentiate. Consequently, we made the decision to exclude the perennial

type, leaving us with the remaining five types as our final functional group categories for the Random Forest Classification model.

3.3.2 Time-series Analysis and Amplified Response Analysis

In order to distinguish different functional groups and try to differentiate grass species classes using knowledge of phenological cycles in the region, we constructed several time-series of NDVI and MSAVI2 from 2013 to 2023 using Landsat 8 OLI and Sentinel-2 MSI data. We used training data to extract mean and median vegetation indexes values from each of the polygons and generate time-series curves using custom Python scripts. In addition, yearly and monthly statistics with standard deviation were calculated and visualized to understand the degree of overlap between classes and the ability to distinguish them using vegetation indexes.

We explored another promising time-series analysis technique for identifying specific growth responses of invasive species in relation to precipitation trends. This response, commonly seen as an amplified growth of cheatgrass in response to an increased mean precipitation, was noticed by several researchers (Hellman et al., 2004; Brown et al., 2015; Blair et al., 2016). The authors found that cheatgrass-dominated areas showed a significantly amplified response to rainfall compared to native shrub/bunch grass areas. This means that cheatgrass is more likely to increase in productivity in years with high rainfall, producing high NDVI and MSAVI2 values, and decrease in productivity in years with low rainfall, providing low NDVI and MSAVI2 values. Our team investigated the potential for this method to distinguish cheatgrass or annual grasses from other landcover types. To test this response, we generated box and whisker plots for each year in the study period and overlaid it with mean yearly precipitation data collected from PRISM dataset in addition to time-series plots.

3.3.3 Random Forest

Random Forest has proven to be one of the most effective models for land cover classification tasks (Rodriguez-Galiano et al., 2012). Therefore, we employed it to generate classification maps for five categories: grass, bare soil, rock, shrub, and tree. Before running the Random Forest, we required two datasets: predictors and training data. The predictors used for the model consisted of topographical variables (elevation, slope, and aspect), indices (NDVI, MSAVI2, NDWI, and BSI), phenological variables (difference of NDVI and MSAVI2), and the bands of Landsat 8 OLI. These predictors were then compiled into one TIFF image by using the Composite Bands geoprocessing tool in ArcGIS Pro. We divided the training data equally into two subsets by using the Subset Features function in ArcGIS Pro: one for training and the other for validation. The training subset was used to train the Random Forest model, while the validation subset was used to validate the performance of the trained model.

Two classification maps for the years 2022 and 2013 were generated using an R package called Random Forest. Initially, we trained the Random Forest model using the predictors in 2022 and the training subset mostly collected after 2020. Subsequently, the trained model was used to produce the classification map for 2022. The next step involved preparing the TIFF image containing the predictors for 2013. We then applied the trained Random Forest model to this data to generate the classification map for 2013.

We generated a probability image as another output of the trained Random Forest model. Using the proportion of decision trees in the Random Forest that vote for a certain class, the model predicts the probability of each pixel belonging to that class. Thus, each pixel stores the probability voted for a specific class. In our case, we were particularly interested in identifying hotspot areas of invasive grass, so the probability map allowed us to highlight these regions.

Given that most of the invasive grass is annual grass, and the grass types in the classification map were trained mostly from our partner's in-situ annual grass data, we assume that the grass type in our classification map is more likely to be annual invasive grass. Based on this assumption, we processed our image to create the annual grass probability map. Firstly, we masked out areas in the classification map for 2022 that are not

grass and overlapped it with the probability image for 2022 in Idrisi TerrSet by using Reclass and Overlay Functions, leaving the probability map for the grass type. Subsequently, we used the Reclassify function in ArcGIS pro to reclassify the probability map, highlighting areas that are most likely to be annual invasive grass.

3.3.4 Confusion Matrix Validation

A confusion matrix is a table used to evaluate the performance of a classification model by comparing predicted land cover types against the actual land cover types. To generate the confusion matrix, we used the Compute Confusion Matrix tool in ArcGIS Pro, which computes a confusion matrix using independent validation points. Initially, we converted a reserved subset of our field data polygons to points by employing the Polygon to Raster tool and then using the Raster to Point tool in ArcGIS Pro. Next, we extracted the classified values of the 2022 classification map for each point. Finally, the confusion matrix was generated by comparing the classified values with the ground truth (known) values for each point. Using the confusion matrix, we could assess the accuracy and performance of the classification model, gaining insights into its ability to correctly classify land cover categories and identify potential errors or biases in the classification results.

3.3.5 Unsupervised Classification

We used the ISO Cluster Unsupervised Classification algorithm tool in ArcGIS Pro to perform unsupervised classification on a Landsat image of area identified as Grass during the Random Forest classification. The goal of the classification was to distinguish between annual & perennial grasses and Bare Soil. The ISO cluster algorithm works by finding clusters of pixels with similar spectral reflectance values. This allowed us to identify groups of pixels that are likely to be the same type of grass or bare soil. The input for the model was the Landsat 8 OLI bands composite used in the Random Forest classification. The initial number of classes was three as an assumption that unsupervised classification could distinguish between desirable classes.

3.3.6 Land Change Modeler

The Land Change Modeler (LCM) is a specialized tool in Idrisi TerrSet designed for land change analysis and prediction. It enables users to analyze and model land cover changes over time, making it a valuable tool for understanding landscape dynamics and developing land use strategies. In the LCM, we input the classification maps for 2013 and 2022 to analyze the land cover changes that occurred over the nine-year period. Additionally, using elevation, slope, and aspect as static variables, the LCM forecasted a potential land cover classification map for the year 2033. This forecasting capability allowed us to project potential land cover changes and aid planning for future land use scenarios.

3.3.7 RAP Accuracy Analysis

Using the comparable classifications of both the RAP and Random Forest classifications as described in 3.2.4, we visually compared the outcomes of our Random Forest classification with the RAP. To do this, we used a false color composite of Landsat imagery as a base map to compare each classification against (Figure C1). This false color composite highlights vegetation in green, making it easier to distinguish vegetation from other land cover types.

The RAP provides an accuracy report for the entire national dataset. In order to generate an accuracy assessment for the RAP that is representative of only CARE, we needed to find a way to test its accuracy ourselves. We determined the accuracy of the 2022 RAP dataset for Capitol Reef by generating a confusion matrix based on the same validation data that we used to validate the Random Forest model. We also determined the agreement between the classifications by generating a confusion matrix between the two classifications (Table C2).

4. Results & Discussion

4.1 Analysis of Results

4.1.1. Random Forest

The random forest model produced a variety of outputs, including the variable importance plot, partial dependence plots, classification maps for 2013 and 2022, and the annual grass probability map for 2022. The variable importance plot illustrates the level of reliance that the random forest classification model places on specific predictors. The plot in our model (Figure D1) is measured by Mean Decrease in Accuracy. A higher value on the right side of the plot indicates greater significance of the predictor for the model. Thus, in our Random Forest model, elevation emerges as the most important predictor, followed by NDVI, slope, MSAVI2, and MSAVI2 difference.

The partial dependence plots offer a means to visualize the connection between a particular classification type and its significant predictors. A rising curve on the plot signifies a positive relationship between the classification type and a specific predictor, while a declining curve indicates a negative relationship. A flat line, on the other hand, reflects no discernible relationship. The partial independence plots (Figure D2) indicate the correlation between the “Grass” class and its six most vital predictors. In essence, these plots indicate that grass demonstrates a negative correlation with elevation, NDVI, and MSAVI2. Conversely, it exhibits a positive relationship with the aerosol band of Landsat 8 OLI, NDVI difference, and MSAVI2 difference.

Upon training the Random Forest classifier, we generated classification maps for the years 2013 and 2022. A discernible pattern emerged as we observed that the western region of Capitol Reef National Park features more vegetation, including shrubs and trees, compared to the eastern part. Increased grass growth is noticeable in the southern-eastern quadrant, while the northeastern area primarily comprises bare soil and rocks. Similarly, in our analysis of 2013–2022 land change, notable trends became apparent. Grass, bare soil, and rock categories observed increases of 0.11%, 1.99%, and 3.97%, respectively. In contrast, there was a decrease in shrub and tree coverage by 2.4% and 3.67%, respectively, signifying alterations in vegetation distribution over this period. The confusion matrix provided a breakdown of the model's correct and incorrect classifications. Extracting insights from the confusion matrix (Table D4), we discerned that bare soil, rock, and tree categories exhibit higher producer's and user's accuracy, all surpassing 90%. Conversely, grass and shrub types manifested comparatively lower accuracy, registering below 90%. This discrepancy suggests that grass and shrub classifications are more susceptible to misclassification as other categories, such as bare soil and trees. Considering the holistic view, the model demonstrated an impressive overall accuracy of 92.17% and a kappa coefficient of 0.90 (Table D3).

The probability map (Figure D4) has been reclassified into four distinct levels: 22%–43%, 43%–55%, 55%–70%, and 70%–100%. Elevated values on this map signify areas where the likelihood of annual grass occurrence is higher. Consequently, regions depicted in red denote the annual grass hotspot zone, predominantly positioned along the southeastern section of the national park. Furthermore, given the similarity in biological attributes between annual grass and perennial grass, we hypothesize that areas displaying lower probabilities might correspond to perennial grass coverage.

4.1.2 Time-series Analysis and Amplified Response Analysis

Upon a thorough examination of the dataset from 2013 to 2023, our findings did not align with the previously documented amplified growth response of cheatgrass in relation to precipitation trends (Figure E1). A closer look at the box and whiskers plots for the study period overlaid with precipitation data did not show significant change in the values for the wet years. Besides that, it revealed potential overlap between NDVI and MSAVI2 values for the different types of invasive species and functional groups.

A closer look at the time-series data revealed a pronounced bimodal distribution of NDVI values throughout the year (Figure E2). This bimodal pattern was consistent with the wet season post-winter and the monsoon season in late summer and early fall. However, our efforts to study phenological cycles did not identify any specific patterns unique to invasive grasses. These species did not exhibit distinct characteristics that would set them apart from each other or from certain functional groups, such as bare soil. This challenge was further highlighted by the histograms of NDVI values (Figure 3), which showed a significant overlap between the groups, making it even more challenging to distinguish between them. However, we discovered that the

difference in NDVI between two profound dates would be beneficial to our analysis. Analyzing mean NDVI values by month for functional classes (Figure B2), we noticed that the NDVI difference of grass type on 8/30/2022 and 5/25/2022 is greater than the difference between other classes. This difference was used as one of the major predictors for the Random Forest Classification model.

One of the primary challenges faced was the substantial overlap and intersections between the groups (Figure E2). This made it difficult to achieve clear distinctions based solely on vegetation indices. It can be the result of complexities due to class mixing. The presence of mixed pixels, representing areas with a combination of different land cover types, was not fully considered in our analysis. This oversight is significant, especially since some invasive species grow in patches within native vegetation, adding another layer of complexity to the analysis.

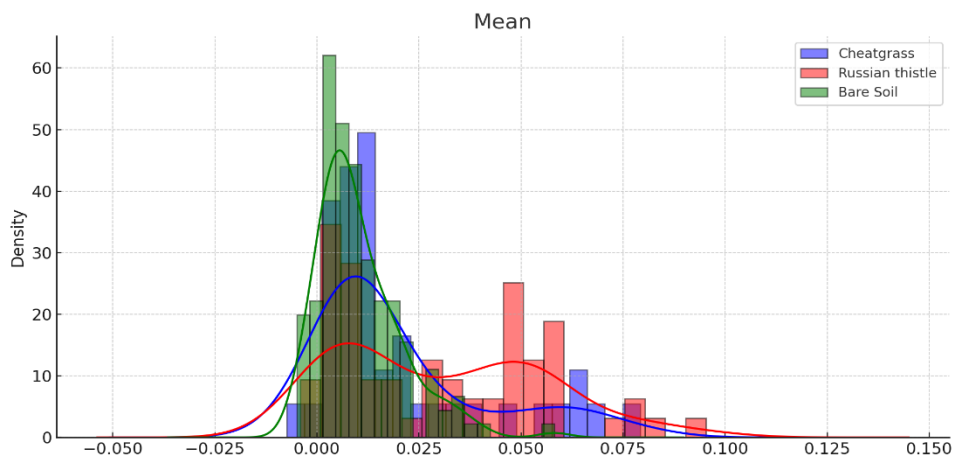


Figure 3. Histograms of the mean NDVI values (x-axis) during the growing period from Sentinel-2 MSI for various functional groups. These histograms indicate overlap in NDVI values among different plant species and functional groups, hindering clear distinction based solely on vegetation indices. The most significant overlap is observed between Bare Soil and cheatgrass, likely due to cheatgrass patches growing on Bare Soil areas during distinct phenological stages.

4.1.3 Unsupervised Classification

After employing the ISO Cluster Unsupervised Classification algorithm in ArcGIS Pro on the Landsat image, the results proved to be inconclusive. Despite the algorithm's ability to identify clusters based on spectral reflectance values, the groups it produced did not provide a clear distinction among the desired classes of annual grasses, perennial grasses, and bare soil (Appendix G). A comprehensive assessment using our training data distribution further underscored this ambiguity. The derived groups could essentially represent any of our functional classes, failing to offer a meaningful separation between them. This outcome underscores the challenges of relying solely on unsupervised classification methods without the support of robust training data or supplementary validation techniques.

4.1.4. Landcover Change Trends and Forecasting

We generated a Random Forest classification map for 2013 with the purpose of detecting land cover change from 2013 to 2022. These findings indicate a trend towards increasing aridity within the study area, which not only diminishes the diversity of plant species, but also reduces the diversity of habitat available for all wildlife in the region. To address our partners interest in visualizing change in vegetation over time, we generated a 10-year projection aimed at forecasting changes within each functional class over the next decade from 2022 to 2033. This 2033 projection relied on the historical trends observed between the 2013 and 2022 classifications (Figure F1).

The forecasted classification map predicts an increased upward trend in grass (+5.64%), bare soil (+1.56%), and rock (+1.77%) cover, and continued degradation of shrub (-6.67%) and tree (-2.02%) cover over the next

10 years (Figure F2). We primarily attribute these changes to the rising temperatures and extended periods of drought. However, it's important to acknowledge that external disturbances could increase the amount of land cover change beyond the predictions outlined by our model. Factors such as climate change, grazing, and fire have the potential to accelerate land cover change within the region.

4.1.5. RAP vs Random Forest

Using the same validation data that we retained for the Random Forest validation, we found that the RAP only has 56% accuracy across the park based on our field data. The cross-tabulation between the RAP and the Random Forest classifications (Table D2) reveals that the RAP classifies 9.9% less grass, 45.63% more bare ground, 34.46% less shrub, and 7.06% less tree than the Random Forest classification did for 2022. Overall, there is only a 47.41% agreement between the two classification methods.

In our comparison between Random Forest and RAP, we noticed the Random Forest classification appears to follow the trends of vegetation in the park more accurately than the RAP classification. Specifically, the RAP seems to misidentify more areas as bare ground and under classifies grasses. Despite the need for better training data, the Random Forest model's high accuracy shows its ability to effectively identify the spectral patterns of grasses, which is crucial for our partners' interests. This indicates that Random Forest may be a more reliable tool for mapping invasive species, especially considering that the RAP model appears to struggle in distinguishing between bare ground and grasses within the park. For a geologically diverse and complicated landscape, we believe that the ability to train the model with local training data rather than regional data is especially advantageous for our study area.

4.2 Feasibility Assessment

Through evaluating our methodology, we are confident in its potential to address our partner's concerns and enhance decision-making processes for our end users. Our project's findings suggest that our partners can benefit from these methods by leveraging Earth observations at a local scale. By integrating Landsat imagery and Random Forest modeling, we have created classification maps that effectively describe vegetation functional groups within CARE. This approach offers a comprehensive representation of the distribution of invasive species over time, aligning precisely with the partner's needs for remotely sensed techniques and enabling the partner to determine the most suitable approach for their decision-making processes. Our methodology demonstrates clear feasibility in addressing the partner's decision-making needs through Earth observations. The tools and insights we have developed can be used to enhance the partner's ability to manage invasive species, make informed choices, and prepare for ecological disruptions.

4.3 Future Work

Generating a classification map that is directly comparable to the RAP would require a more robust set of in-situ data with target features representing greater than 50% cover for perennial grasses, annual grasses, and bare ground. Having this greater confidence in our training sites would limit many of the assumptions we currently have to make regarding the effects of spectral mixing on our model. Additionally, it would be interesting to acquire hyperspectral data and compare its capabilities to those of multi-spectral imagery datasets such as Landsat 8 OLI and Sentinel-2 MSI. Random Forest models can also be easily adjusted to include different predictor variables that may result in more accurate classifications of the park. Despite its limitations, the Random Forest classification maps are useful in generating predictions for expected land cover change and identifying regions where we expect to see the highest probability of annual grasses within CARE. As standalone products, these maps can help inform decisions regarding ecological conservation and vegetation management plans for our partners at CARE.

5. Conclusions

Our project team collaborated with partners at CARE to assess the presence and spread of IEP species. The partners' interest in this project stems from their goal to improve the efficiency and cost-effectiveness of their existing IEP species control strategies. Current practices rely heavily on manual efforts to identify and eradicate these species. However, this project establishes remote sensing-based monitoring methods that can

map vegetation functional groups that are representative of the targeted IEP species. Our data processing workflow involved comprehensive data preparation, image processing techniques, index calculations, classification mapping, and accuracy assessments to obtain reliable and actionable results for ecological monitoring and forecasting. This advanced method will streamline their process by generating products such as vegetation classification maps, land cover change trends, and probability maps, which will further enable them to make informed decisions regarding the best strategies to control IEPs. Our partner can utilize and improve upon the methods we employed to effectively address their challenges and questions about ecological conservation and forecasting in CARE. The remote sensing-based approach offers an effective alternative to conventional methods, enabling better coverage of inaccessible areas and more efficient data collection. By understanding the influential variables and creating functional group classification maps, resource managers can make informed decisions and develop targeted control strategies. However, the challenge of distinguishing between invasive and native grasses requires further investigation and may benefit greatly from the use of high spatial resolution hyperspectral imagery. Overall, this research contributes valuable insights to the ongoing efforts to preserve the ecological integrity of National Parks threatened by invasive exotic plants.

6. Acknowledgements

We would like to thank our partners at NPS CARE: Joseph Ceradini and Morgan Wehtje. We would also like to thank our science advisors: Keith Weber and Joseph Spruce, as well as our DEVELOP Idaho Node Fellow, Ryan Healey

This material contains modified Copernicus Sentinel data (2022), processed by ESA.

This work utilized data made available through the NASA Commercial Smallsat Data Acquisition (CSDA) program. Includes copyrighted material of Planet Labs PBC. All rights reserved.

Any opinions, findings, and conclusions or recommendations expressed in this material are those of the author(s) and do not necessarily reflect the views of the National Aeronautics and Space Administration.

This material is based upon work supported by NASA through contract NNL16AA05C.

7. Glossary

Bands – A segment of the electromagnetic spectrum that a satellite can detect

Clusters – Grouping observations into subsets where members of the same subset share similarities

Confusion matrix – A visual tool showing the discrepancies between actual and predicted classifications

Consumer's Accuracy – Also known as reliability. It's the accuracy rate of classified points truly belonging to their assigned class

Earth observations – Satellites and sensors that collect information about the Earth's physical, chemical, and biological systems over space and time

Invasive species – Species not native to an area that can potentially harm the environment or economy

Kappa coefficient – Measures the agreement level between two sets of data

Landsat – Satellite missions by NASA and the U.S. Geological Survey to observe Earth

LiDAR – Light Detection and Ranging, a system similar to radar but uses laser light

Machine learning – Computers learn from data without explicit programming

Monsoon – A seasonal wind change causing distinct wet or dry periods

MSAVI-2 – Modified Soil Adjusted Vegetation Index, an index to monitor seed growth and its relation to extreme weather

NAIP – National Agriculture Imagery Program, aerial images by the U.S. Department of Agriculture capturing agricultural seasons

Native plant – Plants that have evolved with local wildlife, offering sustainable habitats

NDMI – Normalized Difference Moisture Index, an index to measure vegetation water content

NDVI – Normalized Difference Vegetation Index, an index to estimate vegetation moisture using specific wavelengths

Phenology – Study of natural phenomena in relation to climate and living organisms

PlanetScope – A satellite constellation that captures daily images of Earth's land surface

Producer's Accuracy – The accuracy rate of actual classifications

Random Forest – An algorithm comprising multiple decision trees to make predictions

Remotely-sensed Data – Gathering data about an area from a distance, typically using satellites or aircraft

Sentinel-2 – A European satellite mission designed for high revisit frequency

Time-series – Sequential data points collected over a period

Training Points – Verified data used to assist in supervised classification

Validation – Evaluating a system or software to ensure it meets expectations

Vegetation Indices – Metrics derived from spectral data to provide insights about vegetation

8. References

- Beckie, H. J. & Francis, A. (2009). The biology of Canadian weeds. 65. *Salsola tragus* L. (updated). *Canadian Journal of Plant Science*, 89(7), 75–789. <https://cdnsiencepub.com/doi/pdf/10.4141/CJPS08181>
- Blair, J. M., DiTomaso, J. M., & Hellmann, J. L. (2016). Managing cheatgrass in the sagebrush steppe: A review of current practices and future directions. *Rangeland Ecology & Management*, 69, 557-570.
- Brown, J. A., Svejcar, P. J., Hellmann, J. L., & Abatzoglou, J. T. (2015). Using Random Forest machine learning methods to identify spatiotemporal patterns of cheatgrass invasion through Landsat time series. *Remote Sensing of Environment*, 156, 39-50.
- Copernicus Sentinel-2 MSI (processed by ESA). (2021). MSI Level-2A BOA Reflectance Product. Collection 1. *European Space Agency*. https://doi.org/10.5270/S2_znk9xsj
- Corbin, J. D., & D'Antonio, C. M. (2004). Competition between native perennial and exotic annual grasses: Implications for a historical invasion. *Ecology*, 85(5), 1273-1283.
- Donaldson, S., & Hanson, M. W. (2011). A Northern Nevada Homeowner's Guide to Identifying and Managing Blue Mustard. *University of Nevada, Reno*, FS-11-61. <https://extension.unr.edu/publication.aspx?PubID=3329>
- Gao, B. (1996). NDWI—A normalized difference water index for remote sensing of vegetation liquid water from space. *Remote Sensing of Environment*, 58(3), 257–266. [https://doi.org/10.1016/S0034-4257\(96\)00067-3](https://doi.org/10.1016/S0034-4257(96)00067-3)
- Hellmann, J. L., Kauffman, M. J., & Fahey, T. J. (2004). Identifying land cover variability distinct from land cover change: Cheatgrass in the Great Basin. *Ecological Applications*, 14, 1807-1821.
- Huete, A., Didan, K., Miura, T., Rodriguez, E. P., Gao, X., & Ferreira, L. G. (2002). Overview of the radiometric and biophysical performance of the MODIS vegetation indices. *Remote Sensing of the Environment*, 83(1-2), 195-213.
- Kriegler, F., Malila, W., Nalepka, R., & Richardson, W. (1969). Preprocessing transformations and their effect on multispectral recognition. Proceedings of the 6th International Symposium on Remote Sensing of Environment. *Ann Arbor, MI: University of Michigan*, 97-131.
- National Park Service – Utah. Weather - Capitol Reef National Park. *National Park Service*. <https://www.nps.gov/care/planyourvisit/weather.htm>
- Pavek, D. S. (1992). Halogeton glomeratus. *U.S. Department of Agriculture: Forest Service - Rocky Mountain Research Station: Fire Effects Information System*. <https://www.fs.usda.gov/database/feis/plants/forb/halglo/all.html>
- Peterson, E. B. (2005). Estimating cover of an invasive grass (*Bromus tectorum*) using tobit regression and phenology derived from two dates of Landsat ETM+ data. *International Journal of Remote Sensing*, 26(12), 2491-2507.
- Planet Team. (2017). Planet Application Program Interface: In Space for Life on Earth. San Francisco, CA. <https://api.planet.com>

- Qi, J., Chehbouni, A., Huete, A. R., Kerr, Y. H., & Soroosian, S. (1994). A modified soil adjusted vegetation index. *Remote Sensing of the Environment*, 48(2), 119–126.
- Rodriguez-Galiano, V. F., Ghimire, B., Rogan, J., Chica-Olmo, M., & Rigol-Sanchez, J. P. (2012). An assessment of the effectiveness of a random forest classifier for land-cover classification. *ISPRS journal of photogrammetry and remote sensing*, 67, 93-104.
- USDA Agricultural Research Service. (2023). “Rangeland Analysis Platform.” *USDA ARS*.
<https://rangelands.app/>
- USGS. (2018). National Agriculture Imagery Program (NAIP). [Data set]. USGS EROS Archive.
<https://doi.org/10.5066/F7QN651G>
- USGS. (2020). Landsat 8-9 OLI/TIRS Collection 2 Level-2 Science Products. [Data set]. USGS EROS Archive. <https://doi.org/10.5066/P9OGBGM6>
- USGS n.d. Geology of Capitol Reef National Park. *Geology and Ecology of National Parks*.
<https://www.usgs.gov/geology-and-ecology-of-national-parks/geology-capitol-reef-national-park>
- Witwicki, D. L. (2020). Status and trends in upland vegetation and soils at Capitol Reef National Park, 2009–2018: Natural Resource Report. *National Park Service, Fort Collins, Colorado*.
<https://doi.org/10.36967/nrr-2279505>

9. Appendices

Appendix A

Table A1.

Invasive Species of Interest in Capitol Reef National Park

Scientific name	Common name	Functional Class	Phenology	Morphology
<i>Salsola tragus</i>	Russian thistle	Annual forb	C4 Warm Season	Bushy
<i>Bromus tectorum</i>	Cheatgrass	Annual grass	C3 Cool Season	Bunchgrass
<i>Halogeton glomeratus</i>	Halogeton	Annual forb	May - June	Basal branching stems
<i>Malcolmia africana</i>	African mustard	Annual forb	April - May	Leafy branching forb
<i>Chorispora tenella</i>	Blue mustard	Annual forb	April - May	Leafy spreading forb

Table A2.

Remote sensing platforms and data products utilized for this project

Platform / Sensor	Data product	Spatial / Temporal Resolution	Dates	Acquisition method
Landsat 8 OLI	USGS Landsat 8 Level 2, Collection 2, Tier 1	30-m / 16 days	April 2013 – Present	Accessed through Google Earth Engine tools using custom script
Sentinel-2 MSI	Harmonized Sentinel-2 Multispectral Instrument, Level-2A	10-m / 5 days	2019 – Present	Accessed through Google Earth Engine tools using custom script
Planet	PlanetScope SuperDove 8 Band imagery	~ 1-3 m / ~1-2 days	2019 – Present	Obtained and downloaded through Planet Explorer and processed through Google Earth Engine and ArcGIS Pro

Table A3.

List of datasets used for the project

Source	Data product	Usage	Acquisition method
USGS	2019 Kane County Lidar Elevation Data: QL 2 1-meter Lidar 2 ppm 2020 Southern Utah Lidar Elevation Data: QL 2 1-meter Lidar 2 and 8 ppm	Provide high resolution topographic data of partial extent study area	Accessed and downloaded through USGS Lidar explorer and processed in ArcGIS Pro
National Agriculture Imagery Program	National Agriculture Imagery Program (NAIP) Digital Ortho quarter quads (DOQQ) 1-m resolution imagery	Fine spatial-resolution imagery to aid in distinguishing ground features and georectification	Accessed and downloaded through Google Earth Engine tools using a custom script and processed in both Google Earth Engine and ArcGIS Pro

Table A4.

Spectral band calculations for generating vegetation indices used in the Random Forest model. Bands include near-infrared (NIR), red, green, blue, and shortwave infrared (SWIR). Indices used include the Normalized Difference Vegetation Index (NDVI), Enhanced Vegetation Index (EVI), Modified Soil Adjusted Vegetation Index (MSAVI), and Normalized Difference Moisture Index (NDMI).

Index	Equation	Purpose and Reference
NDVI	$\frac{NIR - Red}{NIR + Red}$	Detection of live green vegetation (Kriegler et al., 1969)
EVI	$Green \times \frac{NIR - Red}{NIR + 6 \times Red - 7.5 \times Blue + 1}$	Detection of live green vegetation with improved sensitivity in high biomass areas (Huete et al., 2002)
MSAVI2	$\frac{2(NIR + 1) - \sqrt{((2 \times NIR + 1)^2 - 8(NIR - Red))}}{2}$	Soil-adjusted detection of vegetation in arid areas (Qi et al., 1994)
NDMI	$\frac{NIR - SWIR1}{NIR + SWIR1}$	Detection of changes in water content in leaves (Gao, 1996)

Appendix B.

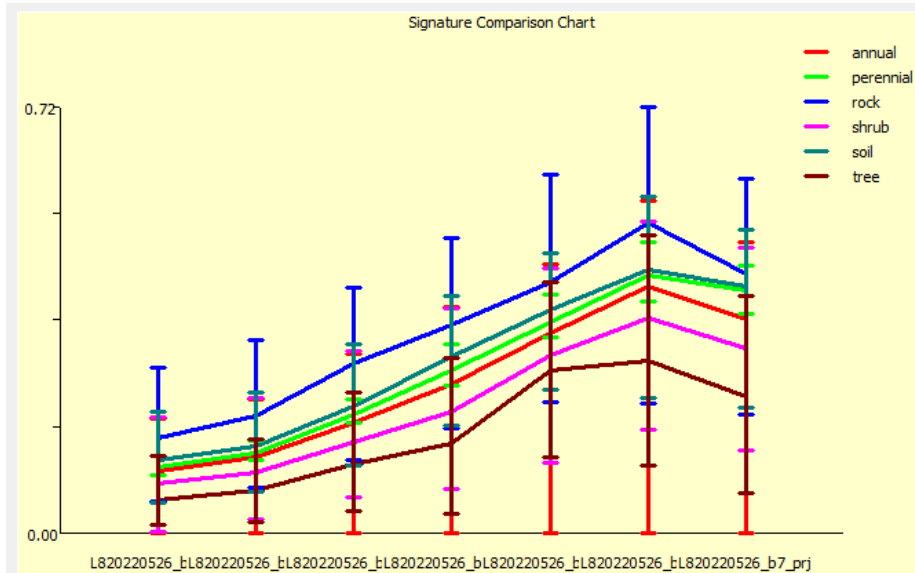


Figure B1. Spectral Signature Chart of 6 types (annual grass, perennial grass, rock, shrub, bare soil, and tree) in Landsat 8 OLI imagery. The distinguishability of spectral signatures plays a crucial role in the accuracy of supervised classification methods. Rock, shrub, and tree types are distinguishable, while annual grass, perennial grass, and bare soil have similar trends.

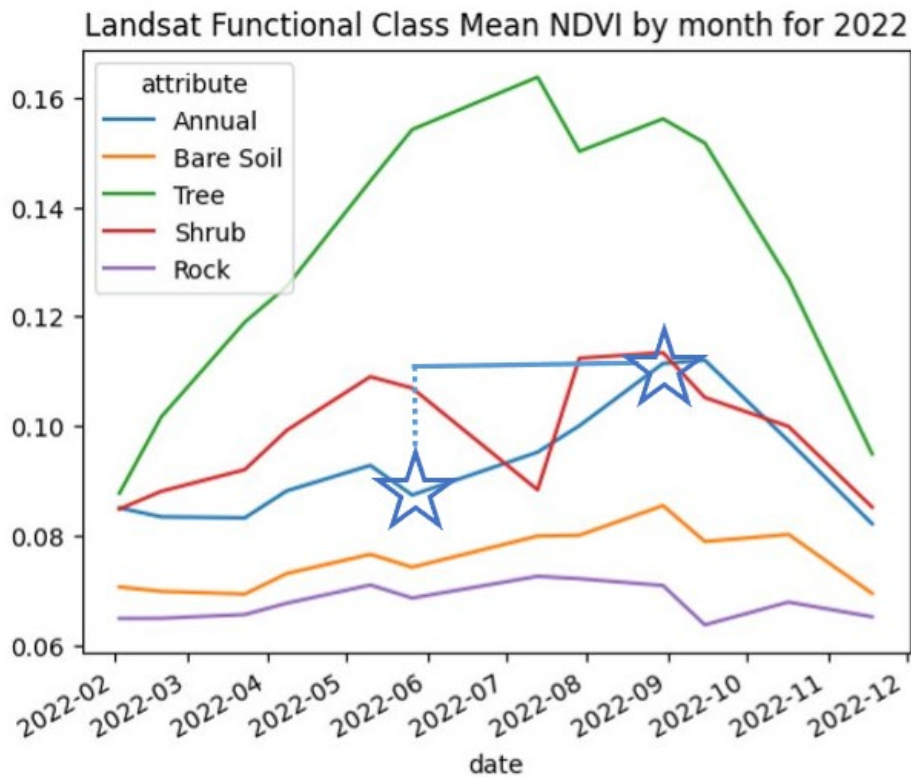


Figure B2. The Landsat 8 OLI Functional Class Mean NDVI by month for 2022. The stars are located at the date we chose for calculating the NDVI difference, where the Annual Grass type has the largest difference of NDVI compared to other types.

Appendix C



Figure C1. Visualization of a Landsat 8 OLI false color composite (Red channel: SWIR-1 band, Green channel: NIR band, Blue channel: Blue band) beside the comparable Random Forest and RAP Classification maps with identical symbology. This visual comparison indicates that the RAP appears to overclassify bare ground and under classifies grasses, while the Random Forest classification appears to overclassify shrub and under classify bare ground. With grasses being the main target of these classification maps, Random Forest proves to be a more suitable tool for this research scope.

Table C2.

Cross tabulation showing the agreements between the Random Forest and RAP classification maps for 2022. The discrepancy in the agreement reveals that the RAP classifies 9.9% less grass, 45.63% more bare ground, 34.46% less shrub, and 7.06% more tree than the Random Forest classification did for 2022. Overall, there is only a 47.41% agreement between the two classification methods.

Method:	RAP					
Class:	Annual	Bare ground	Shrub	Tree	Total:	
RF	Annual	0.31%	11.01%	0.25%	0.23%	11.81%
	Bare ground	0.57%	42.74%	1.72%	0.60%	45.63%
	Shrub	0.86%	27.88%	2.05%	7.85%	38.64%
	Tree	0.17%	1.28%	0.16%	2.31%	3.93%
	Total:	1.91%	82.92%	4.18%	10.99%	100%

Appendix D

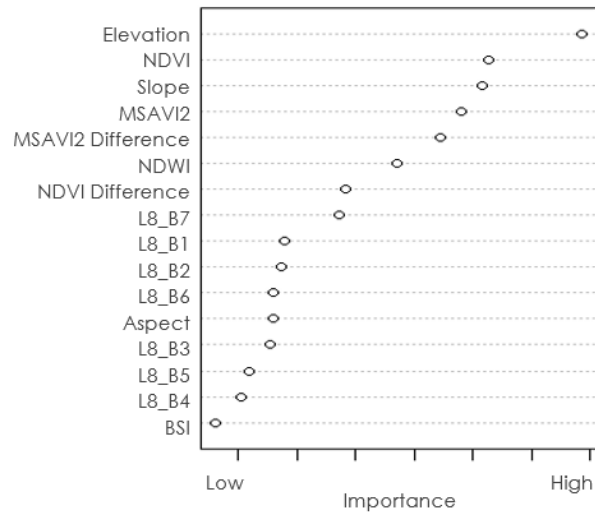


Figure D1. A plot describing the variable importance of predictors fed into the Random Forest Model. Higher values on the right side of the plot indicate greater significance of the predictor for the model. Importance is measured by determining the mean decrease in accuracy if the predictor variable was removed from the classification. The most important predictor variables within our classification model were Elevation, NDVI, Slope, and MSAVI2.

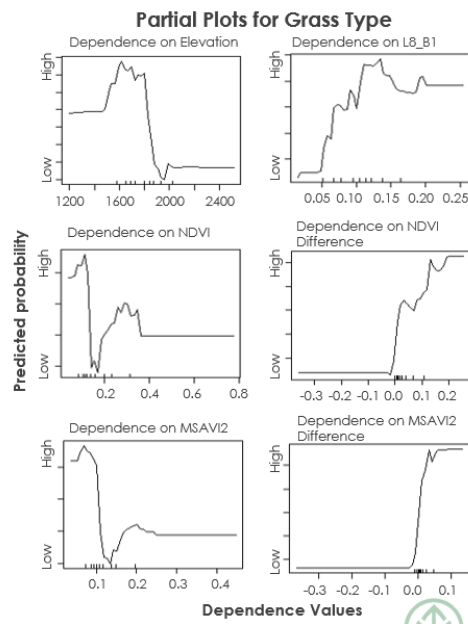


Figure D2. Partial Dependence Plot for the Grass Type. A rising curve on the plot signifies a positive relationship between the grass type and a specific predictor, while a declining curve indicates a negative relationship. In general, Grass has a positive relationship with the first band (the Aerosol Band) of Landsat 8 OLI imagery, NDVI difference and MSAVI2 difference, while it has a negative relationship with elevation, NDVI and MSAVI2.

Table D3.

Confusion matrix for the accuracy of the Random Forest model (overall accuracy: 92.17%, kappa: 0.90)

Ground Truth Classified	Grass	Bare Soil	Rock	Shrub	Tree	Total	Accuracy
Grass	118	10	1	8	0	137	86.13%
Bare Soil	7	189	1	1	0	198	95.45%
Rock	5	3	184	0	0	192	95.83%
Shrub	2	0	5	117	14	138	84.78%
Tree	2	0	0	7	169	178	94.94%
Total	134	202	191	133	183	843	
Accuracy	88.06%	93.56%	96.34%	87.97%	92.35%		92.17%

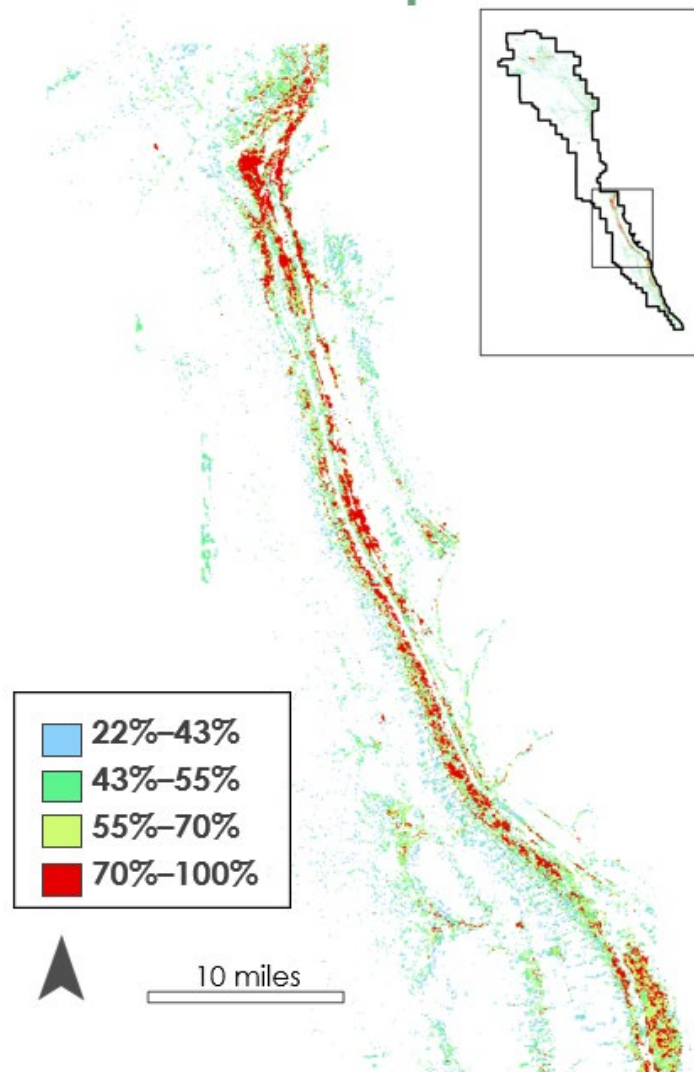


Figure D4. A map of annual grass probability for 2022. Regions depicted in red (70%–100%) denote the regions within the grass classification that are mostly likely to be annual invasive grasses based on our training data.

Appendix E

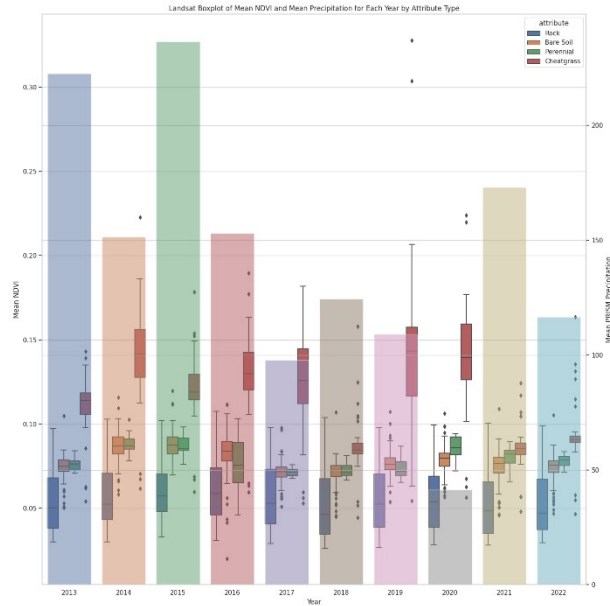


Figure E1. Functional group response to precipitation: The bars represent the mean annual precipitation for CARE throughout the study period. The boxplots, complete with whiskers, display the mean NDVI values during the growing season for different functional groups and certain extracted invasive species. Despite previous research suggesting an amplified response, there's no clear correlation between precipitation amounts and NDVI values for cheatgrass and other types. Additionally, the graph shows some overlap among various functional groups.

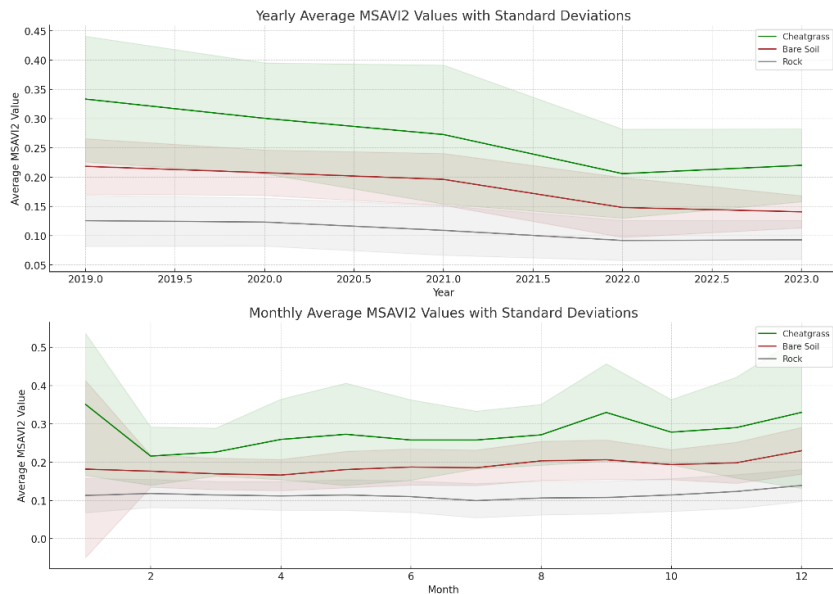


Figure E2. Yearly and monthly average MSAVI2 values for cheatgrass and certain functional groups, accompanied by standard deviations, are presented. Cheatgrass exhibits two distinct peaks around May and September, aligning with the area's bimodal precipitation patterns. The standard deviations reveal a substantial overlap in values for the majority of the growing season.

Appendix F

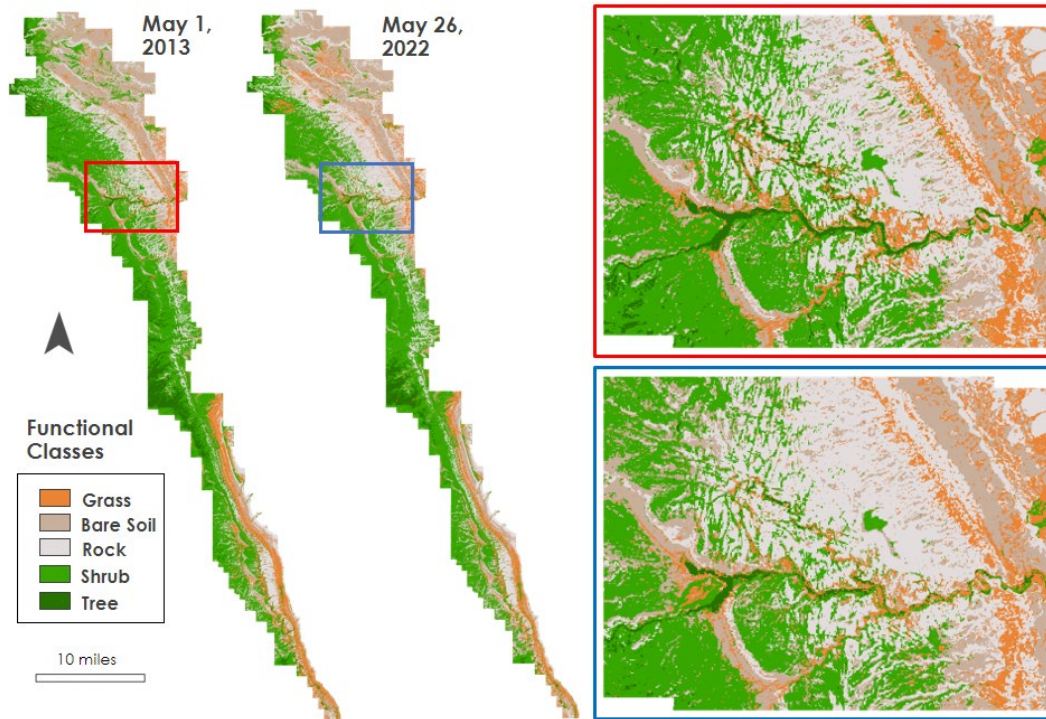


Figure F1. The results of the Random Forest classification for 2013 and 2022. Grass, bare soil, and rock categories have observed increases of 0.11%, 1.99%, and 3.97%, respectively. In contrast, there is a decrease in shrub and tree coverage by 2.4% and 3.67%, respectively.

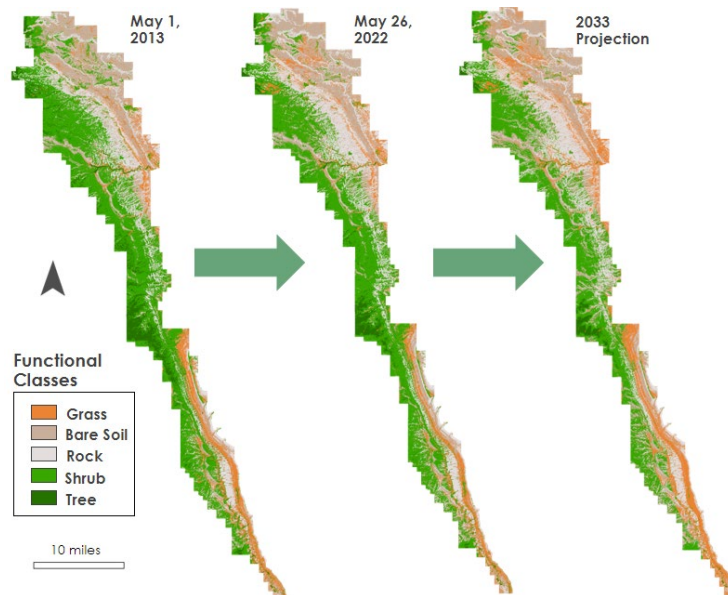


Figure F2. The results of the Random Forest classifications for 2013, 2022, and the forecasted map of 2033. The forecasted classification map predicts an increased upward trend in grass (+5.64%), bare soil (+1.56%),

and rock (+1.77%) cover, and continued degradation of shrub (-6.67%) and tree (-2.02%) cover over the next 10 years.